npj | Computational Materials

www.nature.com/npjcompumats

ARTICLE OPEN

Interplay between Kitaev interaction and single ion anisotropy in ferromagnetic CrI_3 and $CrGeTe_3$ monolayers

Changsong Xu[1], Junsheng Feng[2,3], Hongjun Xiang[2,4] and Laurent Bellaiche[1]

Magnetic anisotropy is crucially important for the stabilization of two-dimensional (2D) magnetism, which is rare in nature but highly desirable in spintronics and for advancing fundamental knowledge. Recent works on CrI_3 and $CrGeTe_3$ monolayers not only led to observations of the long-time-sought 2D ferromagnetism, but also revealed distinct magnetic anisotropy in the two systems, namely Ising behavior for CrI_3 versus Heisenberg behavior for $CrGeTe_3$. Such magnetic difference strongly contrasts with structural and electronic similarities of these two materials, and understanding it at a microscopic scale should be of large benefits. Here, first-principles calculations are performed and analyzed to develop a simple Hamiltonian, to investigate magnetic anisotropy of CrI_3 and $CrGeTe_3$ monolayers. The anisotropic exchange coupling in both systems is surprisingly determined to be of Kitaev-type. Moreover, the interplay between this Kitaev interaction and single ion anisotropy (SIA) is found to naturally explain the different magnetic behaviors of CrI_3 and $CrGeTe_3$. Finally, both the Kitaev interaction and SIA are further found to be induced by spin–orbit coupling of the heavy ligands (I of CrI_3 or Te of $CrGeTe_3$) rather than the commonly believed 3*d* magnetic Cr ions.

npj Computational Materials (2018)4:57 ; doi:10.1038/s41524-018-0115-6

INTRODUCTION

Two-dimensional (2D) magnetic materials are receiving a lot of attention, due, e.g., to the search for long-range ferromagnetism (FM),[1,2] which can facilitate various applications from sensing to data storage.[3,4] According to Mermin and Wagners theorem,[2] however strong the short-range isotropic couplings are, the realization of 2D magnetism relies on magnetic anisotropy, as a result of spin–orbit coupling (SOC). The requirement of strong magnetic anisotropy in low-dimensional systems therefore explains the rareness of 2D FM materials.

The recent observation of FM in monolayers made of CrI_3 and $CrGeTe_3$,[5–7] therefore opens a new chapter in the field of 2D materials. The chromium in both compounds share the same valence state of Cr^{3+}, with the $3d^3$ configuration and $S=\frac{3}{2}$.[7–10] FM arises there from the super exchange between nearest-neighbor Cr ions, that are linked by I or Te ligands through nearly 90° angles.[10,11] CrI_3 has been demonstrated to be well described by the Ising behavior,[1,5,12] for which the spins can point up and down along the out-of-plane *z*-direction. In contrast, the magnetic anisotropy of $CrGeTe_3$ was determined to be consistent with the Heisenberg behavior,[2,7,12] for which the spins can freely rotate and adopt any direction in the three-dimensional space. Interestingly, structural and electronic similarities between these two compounds strongly contrast with their difference in magnetic behaviors, which implies subtle origins for their magnetic anisotropy. A recent theoretical work adopted the XXZ model, for which the exchange coupling is identical between the in-plane *x*-direction and *y*-direction but different along the out-of-plane *z*-direction, to explain the out-of-plane magnetization of CrI_3.[8] However, there is no definite proof that the XXZ model is accurate enough to describe the magnetic anisotropy of CrI_3, and there is a current paucity of knowledge for the mechanism responsible for the magnetic anisotropy of $CrGeTe_3$. Hence, a thorough microscopic understanding of the difference between the Ising behavior of CrI_3 and the Heisenberg behavior of $CrGeTe_3$ is highly desired.

In particular, it is tempting to investigate if the Kitaev interaction,[13] which is a specific anisotropic exchange coupling, can also be significant in CrI_3 and $CrGeTe_3$. This temptation is mainly based on the fact that these two materials adopt a honeycomb lattice and edge-sharing octahedra, exactly as the layered Na_2IrO_3 and *a*-$RuCl_3$ compounds which exhibit magnetic behaviors that are close to spin liquids[14]—as a result of significant Kitaev interactions. Interestingly, finding finite Kitaev interaction in Cr-3*d*-based CrI_3 and $CrGeTe_3$ compounds would enlarge the types of systems possessing such interaction, not only from 4*d* or 5*d* to 3*d* transition-metal-based insulators, but also from $S=1/2$ to $S=3/2$ systems. Such broadening is in-line with recent theoretical predictions of Kitaev interaction in d^7 or 3*d* systems.[15,16]

The main goal of this manuscript is to report results of first-principles calculations, along with the concomitant development of a simple but predictive Hamiltonian, to demonstrate that: (i) significant Kitaev interaction does exist in CrI_3 and $CrGeTe_3$ (which also invalidates the XXZ model in these two compounds); and (ii) the different interplay between this Kitaev interaction and the single ion anisotropy (SIA) naturally explains the observed magnetic anisotropy in these 2D ferromagnetic materials. Another surprising result is that the Kitaev and SIA anisotropies are both dominantly induced by the SOC of the heavy ligand elements rather than the 3*d* element Cr.

[1]Physics Department and Institute for Nanoscience and Engineering, University of Arkansas, Fayetteville, AR 72701, USA; [2]Key Laboratory of Computational Physical Sciences (Ministry of Education), State Key Laboratory of Surface Physics, and Department of Physics, Fudan University, 200433 Shanghai, China; [3]School of Physics and Materials Engineering, Hefei Normal University, 230601 Hefei, China and [4]Collaborative Innovation Center of Advanced Microstructures, 210093 Nanjing, China
Correspondence: Hongjun Xiang (hxiang@fudan.edu.cn) or Laurent Bellaiche (laurent@uark.edu)

Received: 30 June 2018 Accepted: 11 October 2018
Published online: 05 November 2018

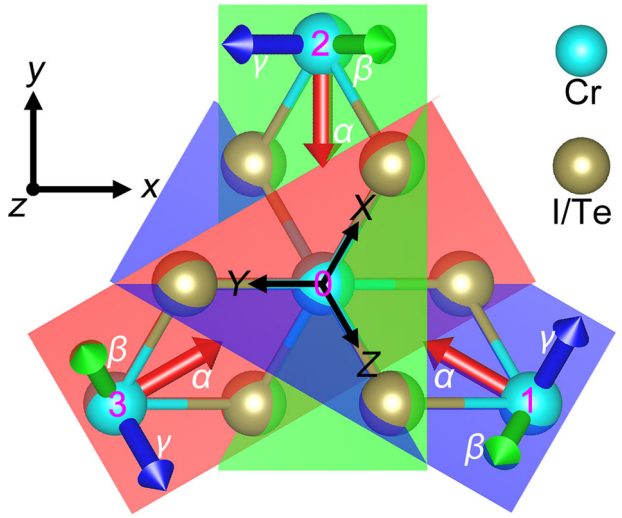

Fig. 1 Schematization of the CrI_3 and $CrGeTe_3$ structures, as well as the different coordinate systems indicated in the text. The planes in blue, green and red indicate the easy plane form Kitaev interaction for Cr0-Cr1, Cr0-Cr2 and Cr0-Cr3 pairs, respectively. Note that Ge of $CrGeTe_3$ is not shown for simplicity

RESULTS

Magnetic Hamiltonian and coupling coefficients

To precisely describe the magnetic anisotropy and explore differences between CrI_3 and $CrGeTe_3$, we consider a Hamiltonian containing both exchange coupling, $\mathcal{H}_{ex}$, and SIA, $\mathcal{H}_{si}$, terms:

$$\mathcal{H} = \mathcal{H}_{ex} + \mathcal{H}_{si} = \frac{1}{2}\sum_{i,j} S_i \cdot \mathcal{J}_{ij} \cdot S_j + \sum_i S_i \cdot \mathcal{A}_{ii} \cdot S_i \quad (1)$$

where $\mathcal{J}_{ij}$ and $\mathcal{A}_{ii}$ are 3×3 matrices gathering exchange and SIA parameters, respectively. The sum over i in Eq. (1) runs over all Cr sites, while the sums over i, j run over all nearest-neighbor Cr pairs (note that the anisotropy in exchange coupling between more distant Cr neighbors is at least an order smaller and is thus negligible, see details in Supplementary Table 1). Density functional theory (DFT) calculations are performed on CrI_3 and $CrGeTe_3$ monolayers to extract the components of $\mathcal{J}$ and $\mathcal{A}$ using a precise four-states method[17,18] (see Supplementary Discussion for details). Note that (i) all the results shown below are based on the use of an effective Hubbard $U = 0.5$ eV, unless stated (see the effects of the choice of other U's in Method section); and (ii) the Dzyaloshinski–Moriya (DM) interaction is absent in our studied systems because of the existence of an inversion center between nearest-neighbor Cr ions.[19]

Let us first focus on the exchange coupling $\mathcal{J}$ matrix for CrI_3 and $CrGeTe_3$. The $\mathcal{J}$ matrix is expressed in the {*xyz*} basis, for which the *x*–*y* plane is the film plane while the *z*-axis is the out-of-plane direction of the film. We choose the Cr0–Cr1 pair (see Fig. 1) to calculate the exchange coupling parameters, from which the parameters for Cr0–Cr2 and Cr0–Cr3 pairs can be deduced via three-fold rotational symmetry. It is numerically found that this matrix is symmetric, i.e., $J_{xy} = J_{yx}$, $J_{yz} = J_{zy}$, and $J_{xz} = J_{zx}$, which is consistent with the fact that there is no DM interaction in our investigated compounds. As shown in Table 1, J_{xx}, J_{yy}, and J_{zz} of CrI_3 possess quite different values of −2.29, −1.93, and −2.23 meV, respectively, while the off-diagonal elements of $\mathcal{J}$ in the {*xyz*} basis are smaller but non-negligible. Such results contrast with the XXZ model adopted in ref. [8], which assumes that (i) $J_{xx} = J_{yy} \neq J_{zz}$ and (ii) J_{xy}, J_{yz} and J_{xz} can all be neglected. Different schemes and strategies, such as changing the value of U, using experimental structures rather than the computationally optimized ones and even replacing other Cr ions by nonmagnetic Al, are used to check their influence on J_{xx}, J_{yy}, and J_{zz} of CrI_3. It is numerically found that they all qualitatively give the same results (as detailed in Supplementary Discussion) in the sense that the aforementioned assumption (i) of the XXZ model providing equality between J_{xx} and J_{yy} is not satisfied, which automatically implies that such latter model is not accurate enough to precisely describe magnetic anisotropy in CrI_3 and $CrGeTe_3$ systems.

The symmetric $\mathcal{J}$ matrix is then diagonalized to obtain its eigenvalues (to be denoted as J_α, J_β, and J_γ) and corresponding eigenvectors (to be coined α, β, and γ) for the Cr0–Cr1 pair. As seen in Table 2, J_α and J_β are the strongest eigenvalues in magnitude and are close to each other in CrI_3 (−2.46 and −2.41 meV, respectively), while J_γ is smaller in magnitude by about 1 meV. The same hierarchy exists between J_α, J_β, and J_γ in $CrGeTe_3$, but with J_α and J_β being now stronger in strength (about −6.65 meV), while $J_\gamma = -6.28$ meV is about 0.4 meV smaller in magnitude than the other two exchange coefficients. As shown in Fig. 1, the α-axis points from Cr1 to Cr0 in both systems, and therefore belongs to the *x*–*y* plane. On the other hand, the β-axis is roughly along the direction joining the two ligands bridging Cr0 and Cr1, and thus does not belong to the *x*–*y* plane. Similarly, the γ-axis, which is perpendicular to both the α-axis and β-axis, does not lie in the *x*–*y* plane. It is important to realize that the {$\alpha\beta\gamma$} basis diagonalizing the $\mathcal{J}$ matrix is specific to each considered Cr pairs, unlike the "global" {*xyz*} basis. In other words, the {$\alpha\beta\gamma$} basis differs for the Cr0–Cr1, Cr0–Cr2, and Cr0–Cr3 pairs, as shown in Fig. 1 by means of red, green, and blue arrows.

The $\mathcal{H}_{ex}$ exchange coupling Hamiltonian can now be rewritten, gathering these three local orthogonal {$\alpha\beta\gamma$} coordinate bases (one for each Cr pair) and assuming that $J_\alpha = J_\beta$ (note that it is

Table 1. Matrix components of $\{\mathcal{J}\}$, as well as the *J* and *K* parameters, of the Cr0–Cr1 pair, and the SIA coefficient A_{zz} for the Cr0 ion, as given by DFT calculations with $S = \frac{3}{2}$

	J_{xx}	J_{yy}	J_{zz}	J_{xy}	J_{yz}	J_{xz}
CrI_3	−2.29	−1.93	−2.23	0.3	0.29	0.17
$CrGeTe_3$	−6.54	−6.37	−6.64	0.15	−0.04	−0.02
	J_α	J_β	J_γ	J	K	A_{zz}
CrI_3	−2.46	−2.41	−1.59	−2.44	0.85	−0.26
$CrGeTe_3$	−6.65	−6.63	−6.28	−6.64	0.36	0.25

Corresponding coefficients for the Cr0–Cr2 and Cr0–Cr3 pairs can be deduced via three-fold rotational symmetry. Note that the global coordinate system {*xyz*} and the local coordinate system {$\alpha\beta\gamma$} of each Cr–Cr pair are shown in Fig. 1. The units of the parameters indicated here is meV.

Table 2. Parameters of Eq. (5) and $\Delta\varepsilon$ from both Eq. (5) and DFT for CrI_3 and $CrGeTe_3$

	Parameters (meV)			$\Delta\varepsilon$ (meV/f.u.)	
	bK	$\frac{2}{3}A_{zz}$	$bK + \frac{2}{3}A_{zz}$	Eq. (5)	DFT
CrI_3	−0.16	−0.17	−0.33	−1.11	−0.82
$CrGeTe_3$	−0.17	0.17	−0.003	−0.01	0.02

$\Delta\varepsilon$ defines the energy difference between the energy for an out-of-plane magnetization and the averaged energy of ferromagnetic states having in-plane magnetization

different with $J_{xx} = J_{yy}$ in XXZ model[8]), as

$$\begin{aligned}\mathcal{H}_{\rm ex} &= \tfrac{1}{2}\sum_{i,j}\left(J_\alpha S_i^\alpha S_j^\alpha + J_\beta S_i^\beta S_j^\beta + J_\gamma S_i^\gamma S_j^\gamma\right)\\ &= \tfrac{1}{2}\sum_{i,j}\left(J\mathrm{S}_i\cdot\mathrm{S}_j + KS_i^\gamma S_j^\gamma\right)\end{aligned} \quad (2)$$

where $J = J_\alpha = J_\beta$ is the isotropic exchange coupling and $K = J_\gamma - J_\alpha > 0$ is the so-called Kitaev interaction that characterizes the anisotropic contribution. Table 1 provides the values of both J and K and, in particular, indicates that the Kitaev interaction cannot be neglected in CrI_3 and $CrGeTe_3$.

Let us now investigate the other energy of Eq. (1), that is the SIA, which involves the $\mathcal{A}$ matrix. For that, one needs to go back to the global {xyz} basis, since only the A_{zz} term can be finite by symmetry. It is numerically found that $A_{zz} = -0.26$ meV in CrI_3, while it adopts a similar magnitude but with a change of sign in $CrGeTe_3$ (since $A_{zz} = 0.25$ meV there). Such significant values of A_{zz} (which is of the same order of magnitude than the K Kitaev parameter) implies that SIA is not negligible, which contrasts with the results in ref. [8]. $\mathcal{H}_{\rm si}$ can thus be simplified as

$$\mathcal{H}_{\rm si} = \sum_i A_{zz} S_i^z S_i^z \quad (3)$$

The total Hamiltonian of Eq. (1) can then be rewritten by combining Eqs. (2) and (3) as

$$\mathcal{H} = \frac{1}{2}\sum_{i,j}\left(J\mathrm{S}_i\cdot\mathrm{S}_j + KS_i^\gamma S_j^\gamma\right) + \sum_i A_{zz} S_i^z S_i^z \quad (4)$$

This simplified Hamiltonian gathers (i) isotropic exchange coupling from J; (ii) anisotropic Kitaev interaction from K in the different local {$\alpha\beta\gamma$} bases; and (iii) SIA in the global {xyz} basis. Let us now try to express the total energy associated with magnetism in an unified coordinate system. Equation (4) shows that the anisotropic part of the exchange energy (arising from K) is only related to the projections of spins on the three different γ axes (one for each Cr–Cr pair). Due to the fact that these three γ axes (to be denoted as γ_1, γ_2, and γ_3, respectively) are normally not perpendicular to each other, we now orthogonalize them using the Löwdin's symmetric orthogonalization scheme.[20] The resulting orthogonal axes form the {XYZ} coordinate system that is shown in Fig. 1. In this global {XYZ} basis, the out-of-plane z-axis of the film is along the [111] direction, and γ_1, γ_2, and γ_3 can be expressed as (1, a, a), (a, 1, a), and (a, a, 1), where $a \in [-\frac{1}{2}, 1]$. As consistent with the relatively large-in-magnitude and negative value of the isotropic exchange coupling J (see Table 1), ferromagnetic states are considered here. When expressing their spin in the {XYZ} basis, i.e., $S(S_X, S_Y, S_Z)$, and considering a magnitude $S = \frac{3}{2}$, it is straightforward to prove that the energy per Cr ion associated with Eq. (4) can then be rewritten as

$$\varepsilon = \left(bK + \tfrac{2}{3}A_{zz}\right)(S_X S_Y + S_Y S_Z + S_Z S_X) + C \quad (5)$$

where $b = \frac{a^2+2a}{2a^2+1}$ and $C = \frac{9}{8}(3J + K) + \frac{3}{4}A_{zz}$ are independent of the spin direction (see Supplementary Discussion for details). One can also easily demonstrate that the symmetric form of $(S_X S_Y + S_Y S_Z + S_Z S_X)$ implies that the magnetization within the x–y plane of the film (for which $S_X + S_Y + S_Z = 0$) is fully isotropic. In other words, any direction of the spin within this x–y plane generates the same energy. Note that we further conducted DFT calculations (not shown here) that indeed numerically confirm that such in-plane isotropy is mainly obeyed in CrI_3 and $CrGeTe_3$ (the maximal energetic difference we found between in-plane directions of spins is 0.006 and 0.004 meV/f.u. in CrI_3 and $CrGeTe_3$, respectively), which attests of the relevance and accuracy of the simple Hamiltonian of Eq. (4) and the resulting energy of Eq. (5). Note also that, although such isotropy in the x–y plane is in line with the results of ref. [8], its origin is totally different: here it arises from the Kitaev interaction and its subsequent frustration, while in ref. [8] the isotropy in the x–y plane lies in the assumption of the XXZ model (see a detailed comparison between the two models in Supplementary Discussion).

It is also worthwhile to emphasize that ref. [8] assumed that SIA is negligible small, while according to Eq. (5) and as we will show below, both the Kitaev interaction (K) and SIA (A_{zz}) play an important role on the overall magnetic anisotropy of CrI_3 and $CrGeTe_3$. To demonstrate such fact, one can realize that Eq. (5) involves $(S_X S_Y + S_Y S_Z + S_Z S_X)$, which adopts (i) its maximum when $S_X = S_Y = S_Z = \frac{\sqrt{3}}{2}$, which corresponds to spins being aligned along the out-of-plane z-direction; *versus* (ii) a minimum when $S_X + S_Y + S_Z = 0$, that is when spins are lying within the x–y plane. The sign and value of the $bK + \frac{2}{3}A_{zz}$ coefficient appearing in front of $(S_X S_Y + S_Y S_Z + S_Z S_X)$ in Eq. (5) should therefore determine the magnetic anisotropy: a negative $bK + \frac{2}{3}A_{zz}$ favors an easy axis along the out-of-plane direction while a positive $bK + \frac{2}{3}A_{zz}$ will encourage spins to lie within the x–y plane. To characterize the strength of such anisotropy between the out-of-plane direction and the x–y plane, we also computed the energy difference, $\Delta\varepsilon$, between the energy of the state having a fully out-of-plane magnetization and the averaged energy of states having in-plane magnetization.

In the case of CrI_3, the b parameter is numerically found to be negative. Together with the positive K and negative A_{zz} from Table 1, both bK and $\frac{2}{3}A_{zz}$ are thus negative. They are determined to be -0.16 and -0.17 meV, respectively, as shown in Table 2. Such negative values indicate that both Kitaev interaction and SIA lead to an out-of-plane easy axis, which is further confirmed by the negative value of -1.11 meV/f.u for $\Delta\varepsilon$, as calculated from Eq. (5). Such value is not only consistent with the result of -0.82 meV/f.u. obtained from DFT calculations (confirming once again the validity and accuracy of our rather simple Eqs. (4) and (5) but also explains the previously determined Ising behavior of CrI_3 favoring the out-of-plane direction for the magnetization.[1,5,12]

In the case of $CrGeTe_3$, the b parameter is also found to be negative and leads to bK adopting a negative -0.17 meV value that is similar to the one of CrI_3. On the other hand, $\frac{2}{3}A_{zz}$ is positive and yields $\simeq 0.17$ meV, which therefore results in a nearly vanishing $bK + \frac{2}{3}A_{zz}$ and thus to a $\Delta\varepsilon$ being nearly zero—that is, -0.01 meV/f.u. according to Eq. (5), which also compares well with the result of 0.02 meV/f.u. directly obtained from DFT (the difference in sign between the energies from Eq. (5) and DFT can be overlooked since both calculations provide vanishing $\Delta\varepsilon$). Such nearly zero value for $bK + \frac{2}{3}A_{zz}$ therefore implies that Eq. (5) predicts that $CrGeTe_3$ is basically isotropic in the whole three-dimensional space, that is any spatial direction of the magnetization (in-plane, out-of-plane or even combination between in-plane and out-of-plane components) should provide similar magnetic energy. Such finding is fully consistent with the observed Heisenberg behavior of $CrGeTe_3$.[2,7,12] Note that, although the isotropic Heisenberg behavior of $CrGeTe_3$ is confirmed by both previous experiments and the present computational work, the anisotropy (Kitaev interaction and SIA) still play a crucial important role in stabilization of the long-range magnetic ground state, as indicated by Mermin and Wagners theorem.[2]

Microscopic origin of Kitaev interaction and SIA

It is also worthwhile to realize that both the Kitaev parameter K and the SIA coefficient A_{zz} originate from SOC. One may wonder what specific ions contribute to such coefficients via SOC. To address such issue, Fig. 2a and b display the atomically resolved contribution of the K parameter as a function of the SOC strength in CrI_3 and $CrGeTe_3$, respectively. Such parameter mainly arises from the SOC of the heavy ligands (namely, I of CrI_3 or Te of $CrGeTe_3$) in a quadratic way, while the SOC of Cr has almost no effect on K (the effect from SOC of Ge on K of $CrGeTe_3$ is also negligible). Such predictions for CrI_3 and $CrGeTe_3$ are consistent

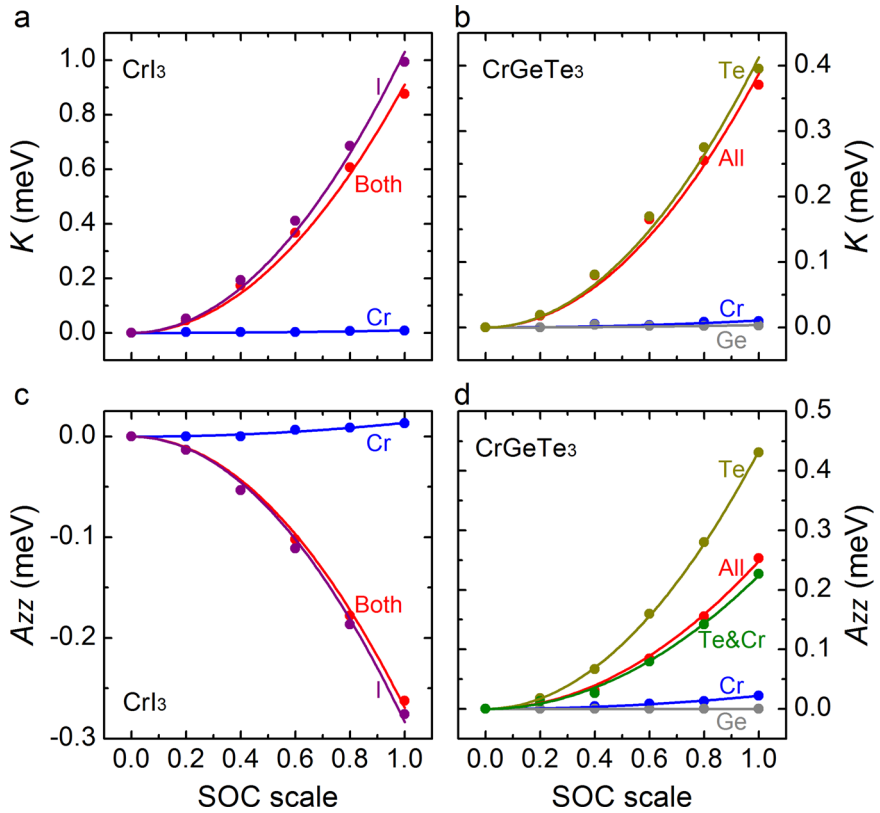

Fig. 2 Atomic dependencies of the Kitaev parameter K and SIA coefficient A_{zz}. Panels **a** and **b** show the dependency of K of CrI_3 and $CrGeTe_3$, respectively, as a function of the SOC strength. Panels **c** and **d** display the dependency of Azz for CrI_3 and $CrGeTe_3$, respectively, as a function of this SOC strength. Note that the value of 1.0 (0, respectively) for this SOC strength corresponds to the actual strength (no SOC, respectively) of the considered element

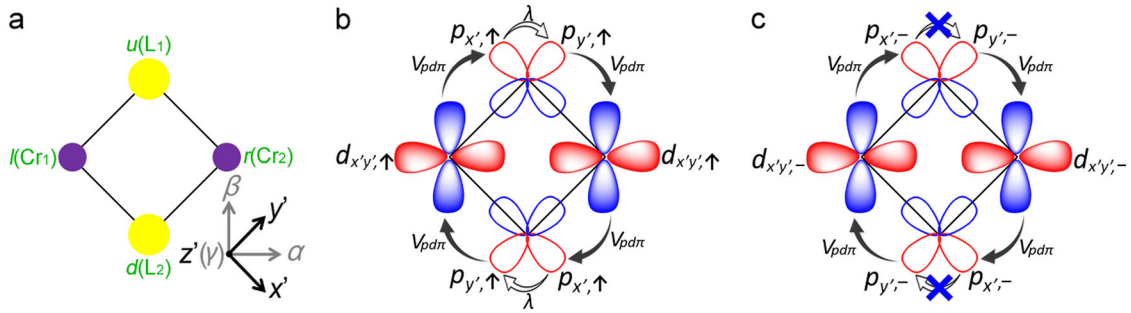

Fig. 3 Tight-binding model and the hooping paths. Panel **a**, the {x′y′z′} coordinate system and the configuration of the considered Cr_2L_2 cluster in the tight-binding model, where L is a ligand ion. Panel **b**, schematization of the extra hopping path related to spins being along the z′ (↑) direction. Panel **c**, the forbidden hopping paths related to spins lying in the x′y′ (−) plane, respectively

with the results of ref. [8] that anisotropy of CrI_3 mainly arises from the SOC of I ligand. This can be understood by the fact that the super exchange between nearest-neighbor Cr sites is mostly mediated by these ligands. To further confirm such results, we developed a tight-binding model (see details in Supplementary Discussion) that contains only two Cr ions and two bridging ligands, which form the $x'y'$ plane (see Fig. 3a for details). Such model confirms that $K > 0$ and $K \propto \lambda^2$, where λ is the SOC strength of ligands.

We now work on understanding the analytical results that $K > 0$ and $K \propto \lambda^2$. If SOC is not considered, the magnetic coupling is isotropic with the strength of J. When the SOC of ligands is included, an extra hopping path emerges for spins that are along the z' direction, as shown in Fig. 3a and b, since $\langle p_{x'\uparrow}|\mathbf{L}\cdot\mathbf{S}|p_{y'\uparrow}\rangle \neq 0$. Such an extra path provides an additional energy term K to the magnetic coupling, as $J_{z'z'} = J + K = \frac{1}{2S^2}(E_{\mathrm{FM},z'} - E_{\mathrm{AFM},z'})$.

In the antiferromagnetic case, the two Cr have opposite spins. The electrons can hop from the occupied t_{2g} orbitals of one Cr to the unoccupied t_{2g} orbitals of another Cr, which can lower the $E_{\mathrm{AFM},z'}$ by the amount of $K \propto \lambda^2$. The form of λ^2 can be understood as that the whole hopping procedure includes two times of ligands' SOC effects, as shown in Fig. 3b. On the other hand, in the ferromagnetic case, t_{2g} orbitals of both Cr are occupied with electrons having the same spin direction. In such case, although the aforementioned extra hopping path still exists, it cannot lead to the energy lowering of $E_{\mathrm{AFM},z'}$. In contrast, there is no such extra hopping path when spins lie in the Cr_2L_2 ($x'y'$) plane (denoted with the "−" mark), since $\langle p_{x'-}|\mathbf{L}\cdot\mathbf{S}|p_{y'-}\rangle = 0$. Such effects are further

illustrated in Fig. 3c. As a result, the total effective $J_{z'z'} = J + K$ is larger than that $J_{x'x'} = J_{y'y'} = J$, i.e., $K > 0$. The findings reported here thus demonstrate, for the first time, that (i) the Kitaev interaction not only exists in 4*d* or 5*d* transition metal insulators, but also can occur in 3*d* systems; and (ii) the SOC of the ligands can play a crucial role on that interaction. Such findings can facilitate the ongoing efforts to realize Kitaev-type interactions in 3*d* systems.[15,16]

Regarding SIA, Fig. 2c shows that the SOC of I is basically responsible for the negative A_{zz} of CrI_3, and that Cr does not significantly contribute to such parameter. Such finding of a ligand-induced SIA is also novel, since SIA is typically believed to arise from the transition metal ion.[21,22] Similarly and as indicated by Fig. 2d, the Te ligand in $CrGeTe_3$ produces a rather strong (and positive, in that case) $A_{z'z'}$ which is even twice as large as the one resulting from the SOC of all considered ions. It is in fact the combination of SOC from both Te and Cr that provides a value of A_{zz} that is close to the total one in $CrGeTe_3$ (note that Ge does not significantely contribute to this total SIA).

DISCUSSION

We now explain on magnetic behaviors of related 2D systems. Another 2D ferromagnetic system, $CrBr_3$, was also studied. It is numerically found (not shown here) that, as similar to CrI_3, both the Kitaev interaction and SIA favor an out-of-plane easy axis in this material. Such finding is consistent with measurements determining that the net anisotropy of $CrBr_3$ is out-of-plane.[23] Interestingly, Eq. (5) of the manuscript can also be useful to shed some light into controversial issues, such as which magnetic model is more pertinent to $CrSiTe_3$. As a matter of fact, early neutron work suggested an Ising-like model[24] for this system, while recent measurements argue between an Heisenberg-like model[25] and an Ising model coupled with long-range interaction.[26] $CrSiTe_3$ shares similarities with $CrGeTe_3$ in the sense that it has a negative bK associated with Kitaev interaction, as well as a positive $\frac{2}{3}A_{zz}$ induced by SIA. However, the former is equal to -0.21 meV and is larger in magnitude than the latter (that is equal to $+0.11$ meV) in $CrSiTe_3$, therefore leading to a less negative $bK + \frac{2}{3}A_{zz}$ of -0.07 meV and thus slightly tipping the balance towards out-of-plane magnetization (as confirmed by our DFT results providing $\Delta\varepsilon = -0.10$ meV for the difference between the energy for an out-of-plane magnetization and the averaged energy of ferromagnetic states having in-plane magnetization). One can thus propose that the correct magnetic model for $CrSiTe_3$ should be related to a slight perturbation of the Ising model, in order to account for possible (weaker) in-plane components of the magnetization in addition to (stronger) out-of-plane ones.

The present general model and the XXZ model are compared here. The present general model (Eqs. (1), (4) and (5)) adopts the most generalized form of the $\mathcal{J}$ and $\mathcal{A}$ matrices, which can capture the microscopic details of different anisotropy. Such model is powerful, as it explains the origin of Kitaev interaction, as well as the competition and collaboration between Kitaev interaction and SIA. It also allows for antisymmetric exchange coupling, i.e. the so-called DM interaction, when the inversion centers between Cr–Cr pair are somehow removed. In contrast, the XXZ model is more macroscopic in nature, since it starts from the overall effects of the frustration among Cr–Cr pairs. Nevertheless, this XXZ model can still somehow describe the competition and collaboration between Kitaev interaction (since J_x and J_z are different from each other) and SIA. As a result, the XXZ model can be technically applied to both CrI_3 and $CrGeTe_3$, as well as to the aforementioned related systems, but, as documented in Section 4 of the Supplementary Discussion, one really has to include SIA there to be more accurate.

Moreover, our work implies potential Kitaev-type quantum spin liquids in related systems. The predicted presence of Kitaev interaction in CrI_3 and $CrGeTe_3$ systems hints towards the possibility of realizing quantum spin liquid state in 3*d* systems. As a matter of fact, further studies we performed indicate that varying in-plane strain can make the isotropic exchange coupling vanishing while the Kitaev interaction remains finite, which is promising to realize quantum spin liquid state in CrI_3 and $CrGeTe_3$ systems. Furthermore, our predictions also provide another way to enhance Kitaev interaction in the "traditional" 4*d* and 5*d* systems, that is, for example, to substitute the light Cl ligand with the heavier I ion in $RuCl_3$ compound. The hybrid source of SOC to produce strong Kitaev interaction should result in interesting physics and phenomena in related systems.

We hope that our first-principles calculations and concomitant development of a simple insightful Hamiltonian (see Eqs. (4) and (5)), along with a tight-binding model, deepens the understanding of magnetic anisotropy in low-dimensional systems. The decomposition of the total magnetic anisotropy into Kitaev and SIA effects further sheds light into the behaviors of other related systems, such as $CrBr_3$ and $CrSiTe_3$, therefore further demonstrating its relevance and importance.

METHODS

DFT parameters

Simulations are performed using the Vienna ab-initio simulation package (VASP).[27] A 350 eV plane wave cutoff energy is used, which is 130% larger than the highest ENMAX of all involved elements. A 12 Å vacuum layer is adopted for all calculations, which is thick enough to get converged results according to former studies.[9,28] The projector augmented wave (PAW) method[29] is employed with the following electrons being treated as valence states: Cr 3*p*, 4*s* and 3*d*, I and Te 5*s* and 5*p*, Ge 4*s* and 4*p*, and Al 3*s* and 3*p*. The local density approximation (LDA)[30] is used, with an effective Hubbard U parameter chosen to be 0.5 eV for the localized 3*d* electrons of Cr ions. Such relatively small U value is based on the facts that (i) the shallow p orbitals of heavy ligands (I or Te) strongly hybridize with 3*d* orbitals of Cr; and (ii) such strong hybridization leads to less localized 3*d* electrons. Nevertheless, other U choices of 0, 1, 2, 4 eV and $U = 4$ eV together with $J = 0.7$ eV are also presently tested and qualitatively render the same results, in the sense that K and A_{zz} have different (the same, respectively) signs for CrI_3 ($CrGeTe_3$, respectively), as shown in Supplementary Table 1. Gaussian smearing with a smearing width of 0.05 meV is used in the Brillouin zone integration. Tetrahedron method with Blöchl corrections is also performed, which yields the same K and A_{zz} (to the precision of 0.01 meV). Note that, exchange couplings between more distant neighbors other than the first nearest neighbors are not considered in the magnetic Hamiltonian, due to the reasons that (i) we focus on the magnetic anisotropy (more distant neighbors may have strong isotropic couplings, but they do not contribute to the stabilization of the long-range order); and (ii) the $\mathcal{J}$ matrix of second nearest neighbors is also calculated (see Supplementary Table 1) and its anisotropy is found to be an order smaller than that of the first nearest neighbors. k-point meshes are chosen, such as they are commensurate with the choice of $4 \times 4 \times 1$ for the unit cell (that contains eight atoms for CrI_3 and 10 atoms for $CrGeTe_3$). For instance, the k-point mesh of a $2 \times 2 \times 1$ supercell is $2 \times 2 \times 1$. Denser k-point meshes up to $4 \times 4 \times 1$ for the $2 \times 2 \times 1$ supercell are also tested and qualitatively yield the same results, as shown in Supplementary Table 2. All magnetic parameters are calculated using the four-state energy mapping method (see Section 3 of Supplementary Discussion for details).[17,18] The Hellman–Feynman forces are taken to be converged when they become smaller than 0.001 eV/Å on each ion. Schematization of crystal structures are prepared using the VESTA software.[31]

DATA AVAILABILITY

All data generated or analyzed during this study are included in this published article (and its supplementary information files).

ACKNOWLEDGEMENTS

We thank Zhenglu Li and Jianfeng Wang for useful discussion. C.X. thanks the support of the Office of Basic Energy Sciences under contract ER-46612. L.B. acknowledges the support of the ARO Grant No. W911NF-16-1-0227. H.X. is

supported by NSFC (11374056), the Special Funds for Major State Basic Research (2015CB921700), Program for Professor of Special Appointment (Eastern Scholar), Qing Nian Ba Jian Program, and Fok Ying Tung Education Foundation. J.F. aknowledges Open Foundation of Key Laboratory of Computational Physical Sciences (Ministry of Education). The Arkansas High Performance Computing Center (AHPCC) is also acknowledged.

AUTHOR CONTRIBUTIONS

C.X. and J.F. contributed equally to this work. H.X and C.X. conceived the idea. H.X. and L.B. supervised this work. C.X. performed the DFT calculations and related analysis, J.F. worked on the tight-binding model. All authors contributed to the discussion of the results and the writing of the manuscript.

ADDITIONAL INFORMATION

Supplementary information accompanies the paper on the *npj Computational Materials* website (https://doi.org/10.1038/s41524-018-0115-6).

Competing interests: The authors declare no competing interests.

Publisher's note: Springer Nature remains neutral with regard to jurisdictional claims in published maps and institutional affiliations.

REFERENCES

1. Griffiths, R. B. Peierls proof of spontaneous magnetization in a two-dimensional Ising ferromagnet. *Phys. Rev.* **136**, A437 (1964).
2. Mermin, N. D. & Wagner, H. Absence of ferromagnetism or antiferromagnetism in one- or two-dimensional isotropic Heisenberg models. *Phys. Rev. Lett.* **17**, 1133 (1966).
3. Soumyanarayanan, A., Reyren, N., Fert, A. & Panagopoulos, C. Emergent phenomena induced by spin-orbit coupling at surfaces and interfaces. *Nature* **539**, 509–517 (2016).
4. Miao, N., Xu, B., Zhu, L., Zhou, J. & Sun, Z. 2D intrinsic ferromagnets from Van der Waals antiferromagnets. *J. Am. Chem. Soc.* **140**, 2417–2420 (2018).
5. Huang, B. et al. Layer-dependent ferromagnetism in a Van der Waals crystal down to the monolayer limit. *Nature* **546**, 270–273 (2017).
6. Gong, C. et al. Discovery of intrinsic ferromagnetism in two-dimensional Van der Waals crystals. *Nature* **546**, 265–269 (2017).
7. Xing, W. et al. Electric field effect in multilayer $Cr_2Ge_2Te_6$: A ferromagnetic 2D material. *2D Mater.* **4**, 024009 (2017).
8. Lado, J. L. & Fernandez-Rossier, J. On the origin of magnetic anisotropy in two dimensional CrI_3. *2D Mater.* **4**, 035002 (2017).
9. Li, X. & Yang, J. $CrXTe_3$ (X = Si, Ge) nanosheets: Two dimensional intrinsic ferromagnetic semiconductors. *J. Mater. Chem. C* **2**, 7071–7076 (2014).
10. Carteaux, V., Brunet, D., Ouvrard, G. & Andre, G. Crystallographic, magnetic and electronic structures of a new layered ferromagnetic compound $Cr_2Ge_2Te_6$. *J. Phys.: Condens. Matter* **7**, 69 (1995).
11. McGuire, M. A., Dixit, H., Cooper, V. R. & Sales, B. C. Coupling of crystal structure and magnetism in the layered, ferromagnetic insulator CrI_3. *Chem. Mater.* **27**, 612–620 (2015).
12. Samarth, N. Condensed-matter physics: Magnetism in flatland. *Nature* **546**, 216–218 (2017).
13. Kitaev, A. Anyons in an exactly solved model and beyond. *Ann. Phys.* **321**, 2–111 (2006).
14. Jackeli, G. & Khaliullin, G. Mott insulators in the strong spin-orbit coupling limit: From Heisenberg to a quantum compass and Kitaev models. *Phys. Rev. Lett.* **102**, 017205 (2009).
15. Liu, H. & Khaliullin, G. Pseudospin exchange interactions in d^7 cobalt compounds: Possible realization of the kitaev model. *Phys. Rev. B* **97**, 014407 (2018).
16. Sano, R., Kato, Y. & Motome, Y. Kitaev-Heisenberg hamiltonian for high-spin d^7 mott insulators. *Phys. Rev. B* **97**, 014408 (2018).
17. Xiang, H., Lee, C., Koo, H.-J., Gong, X. & Whangbo, M.-H. Magnetic properties and energy-mapping analysis. *Dalton Trans.* **42**, 823–853 (2013).
18. Xiang, H., Kan, E., Wei, S.-H., Whangbo, M.-H. & Gong, X. Predicting the spin-lattice order of frustrated systems from first principles. *Phys. Rev. B* **84**, 224429 (2011).
19. Moriya, T. Anisotropic superexchange interaction and weak ferromagnetism. *Phys. Rev.* **120**, 91 (1960).
20. Löwdin, P.-O. On the non-orthogonality problem connected with the use of atomic wave functions in the theory of molecules and crystals. *J. Chem. Phys.* **18**, 365–375 (1950).
21. Xiang, H., Wei, S.-H. & Whangbo, M.-H. Origin of the structural and magnetic anomalies of the layered compound $SrFeO_2$: A density functional investigation. *Phys. Rev. Lett.* **100**, 167207 (2008).
22. Hu, J. & Wu, R. Giant magnetic anisotropy of transition-metal dimers on defected graphene. *Nano Lett.* **14**, 1853–1858 (2014).
23. McGuire, M. A. et al. Magnetic behavior and spin-lattice coupling in cleavable van der waals layered $CrCl_3$ crystals. *Phys. Rev. Mater.* **1**, 014001 (2017).
24. Carteaux, V., Moussa, F. & Spiesser, M. 2D Ising-like ferromagnetic behaviour for the lamellar $Cr_2Si_2Te_6$ compound: A neutron scattering investigation. *Eur. Phys. Lett.* **29**, 251 (1995).
25. Williams, T. J. et al. Magnetic correlations in the quasi-two-dimensional semiconducting ferromagnet $CrSiTe_3$. *Phys. Rev. B* **92**, 144404 (2015).
26. Liu, B. Critical behavior of the quasi-two-dimensional semiconducting ferromagnet CrSiTe3. *Sci. Rep.* **6**, 33873 (2016).
27. Kresse, G. & Joubert, D. From ultrasoft pseudopotentials to the projector augmented-wave method. *Phys. Rev. B* **59**, 1758 (1999).
28. Liu, J., Sun, Q., Kawazoe, Y. & Jena, P. Exfoliating biocompatible ferromagnetic Cr-trihalide monolayers. *Phys. Chem. Chem. Phys.* **18**, 8777–8784 (2016).
29. Blöchl, P. E. Projector augmented-wave method. *Phys. Rev. B* **50**, 17953 (1994).
30. Kohn, W. & Sham, L. J. Self-consistent equations including exchange and correlation effects. *Phys. Rev.* **140**, A1133 (1965).
31. Momma, K. & Izumi, F. VESTA3 for three-dimensional visualization of crystal, volumetric and morphology data. *J. Appl. Crystallogr.* **44**, 1272–1276 (2011).